AIAA-98-4503

Wide-Range Stabilization of an Arm-Driven Inverted Pendulum Using Linear Parameter-Varying Techniques*

Hiroyuki Kajiwara,† Pierre Apkarian,‡ Pascal Gahinet§

Abstract: The purpose of the paper is to demonstrate the ability of LPV (Linear Parameter Varying) control techniques to handle difficult nonlinear control problems. The focus in this paper is on the wide range stabilization of an arm-driven inverted pendulum. Two different LPV control techniques are used to design nonlinear controllers that achieve stabilization of the pendulum over the maximum range of operating conditions while providing time- and frequency-domain performances. The merits of each of these techniques are investigated and the improvements over more classical LTI (Linear Time-Invariant) control schemes such as H_∞ or μ controllers are discussed. A particular emphasis is put on the real-time implementation of these controllers for the inverted pendulum experiment. It is shown that suitable multi-objective extensions of the standard characterization of LPV controllers allow to cope with sampling rate implementation constraints. Finally, a complete validation of the proposed LPV controller structures is carried out through a set of realistic nonlinear simulations but also by means of physical experiment records.

1 Introduction

Gain-scheduling control structures have proved useful in many practical applications. As an example, most aircraft control laws are based on the interpolation of individually designed controllers or make use of some ad-hoc gain-switching policy. Similarly, in robot control problems the controller dynamics are adjusted in real-time according to its geometry and inertias. However, in spite of numerous successful applications, the construction of the overall control structure invariably call for the engineering insights of the designer and more critically, the resulting control laws does not provide any guarantees in face of rapid changes in the scheduled variables. These difficulties have been the main motivation for the development of modern gain-scheduling control techniques and have led leading to some challenging research in the area of the analysis and synthesis of LPV systems. Such systems are described in state-space form as

$$\begin{aligned} \dot{x} &= A(\theta)x + B(\theta)u\,, \\ y &= C(\theta)x + D(\theta)u\,, \end{aligned} \tag{1}$$

where $\theta := \theta(t)$ is a time-varying parameter describing the range of possible dynamics of the plant. Such systems are natural extensions of customary LTI systems. Briefly speaking, the recently available LPV synthesis techniques allow the construction of the global control law as a whole entity for all admissible θ , that is, without requiring unnatural separated design syntheses and furthermore provide theoretical guarantees in terms of both stability and performance in the presence of fast time-domain evolutions of the scheduled variables. Note also that since these synthesis techniques reduce to solving a finite set of LMIs (Linear Matrix Inequality), the underlying computations are both fast and accurate.

In this work, we are considering the challenging application of an Arm-Driven Inverted Pendulum (ADIP) as depicted in Figure 1. The pendulum which is here the top link is driven by the rotated arm (bottom link), instead of a more classical cart. As the arm is rotated and gets closer to the horizontal position, the horizontal motion of the arm tip becomes more limited and the inertias viewed from the arm are modified. This naturally leads to the design of controllers that adjust in real-time to the rotation of the arm. For this purpose, two kinds of LPV synthesis techniques are investigated the so-called LFT and polytopic techniques which use LFT and polytopic representations of the robot, respectively. Our final goal is to completely validate these techniques on the physical experiment. Therefore, in addition

*Copyright ©1997 The American Institute of Aeronautics and Astronautics Inc. All right reserved.

†Kyushu Institute of Technology, 680-4, Kawazu, Iiizuka, 820, Japan. E-mail: kajiwara@ces.kyutech.ac.jp

‡ONERA-CERT, 2 av. Edouard Belin, 31055 Toulouse Cedex, France. E-mail: apkarian@cert.fr

§The MathWorks, Inc., 24 Prime Park Way, Natick, MA 01760. E-mail: pascal@mathworks.com

to the usual stability, performance and robustness requirements, we shall also be concerned by the implementation constraints that inevitably show up in real-world applications. The major implementation constraints are the following.

- The high-frequency gain of the controllers must be compatible with the actuator bandwith.
- The controller dynamics must be consistent with the available sampling rate in this application ($<$ 400 Hz.).

Note that the second of these constraints is especially difficult to handle as it concerns the internal properties of the controller and cannot be directly treated through the properties of the closed-loop system. We shall see however that a suitable multi-objective extension of the polytopic technique provides an effective mean to overcome this difficulty. Another way to handle this implementation constraint would have been to tune the weighting functions until adequate closed-loop plant and open-loop controller specifications are met. However, this procedure revealed to be hardly tractable on this application and in most instances led to high order controllers as it requires complicated weighting functions.

Another important issue is to evaluate the benefits of LPV synthesis techniques in regard to classical robust control techniques such as H_∞ and μ syntheses. It turns out in this application that though the H_∞ and μ controllers are capable of providing some stability guarantees they are, as expected, outperformed by LPV controllers at the performance level.

The paper is organized as follows. Section 2 describes the modeling of the ADIP and introduces the problem specifications. A brief review of the LPV synthesis techniques used for the ADIP is given in Section 3. The full design procedure up to the nonlinear simulations and real experiment results are presented in Section 4. Concluding remarks are given in Section 5.

All LMI-related computations in the application were performed using the LMI Control Toolbox [23], μ controllers were designed using the μ-Analysis and Synthesis Toolbox [22], the nonlinear simulations were obtained using MATLAB/SIMULINK facilities and LPV controllers were implemented using the REAL-TIME WORKSHOP.

For a real symmetric matrix M, the notation $M > 0$ stands for positive definite and means that all the eigenvalues of M are positive. $M < 0$ means all the eigenvalues of M are negative. The upper LFT of $M = \begin{bmatrix} M_{11} & M_{12} \\ M_{21} & M_{22} \end{bmatrix}$ is defined as

$$\mathcal{F}_u(M,K) = M_{22} + M_{21}K(I - M_{11}K)^{-1}M_{12} \quad (2)$$

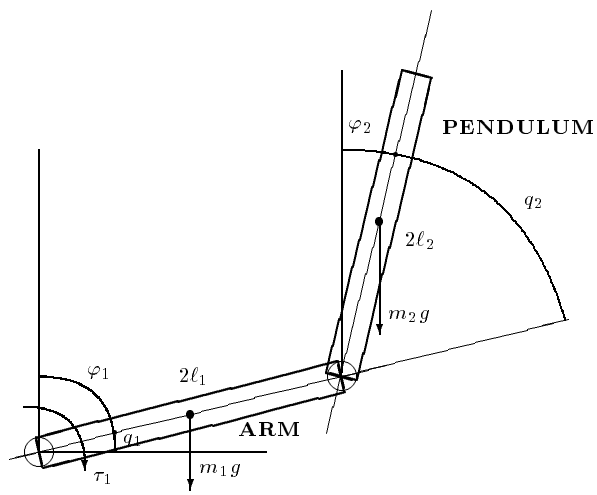

Figure 1: For modeling the ADIP

2 LPV Modeling of the ADIP

In this section, the LPV synthesis model for the ADIP is developed and the design specifications are introduced. Consider the two-link arm depicted in Figure 1. It is well known [1, 2]that the motion equation is described as

$$M(q)\ddot{q} + C(q,\dot{q}) + G(q) = \tau\,, \quad (3)$$

where

$$q = \begin{bmatrix} q_1 \\ q_2 \end{bmatrix} := \begin{bmatrix} \frac{\pi}{2} - \varphi_1 \\ \varphi_1 - \varphi_2 \end{bmatrix}, \quad (4)$$

and

$$M(q) := \begin{bmatrix} M_1 + 2R\cos(q_1) & M_2 + R\cos(q_2) \\ M_2 + R\cos(q_2) & M_2 \end{bmatrix}, \quad (5)$$

$$C(q,\dot{q}) := \begin{bmatrix} -2R\dot{q}_1\dot{q}_2\sin(q_2) - R\dot{q}_2^2\sin(q_2) \\ R\dot{q}_1^2\sin(q_2) \end{bmatrix}, \quad (6)$$

$$M_1 := \frac{4}{3}m_1\ell_1^2 + \frac{4}{3}m_2\ell_2^2 + 4m_2\ell_1^2\,, \quad (7)$$

$$M_2 := \frac{4}{3}m_2\ell_2^2\,, \quad (8)$$

$$R := 2m_2\ell_1\ell_2\,, \quad (9)$$

and

$$G(q) := \begin{bmatrix} -(m_1 + 2m_2)\ell_1 g\cos(q_1) \\ -m_2\ell_2 g\cos(q_1 + q_2) \end{bmatrix}, \quad (10)$$

$$\tau := \begin{bmatrix} -\tau_1 \\ 0 \end{bmatrix} . \tag{11}$$

In this application, the first joint is actuated and the second joint is free. From (3)-(11), we can derive the following equations.

$$\begin{aligned} &(M_1 - M_2)\ddot{\varphi}_1 + R\cos(\varphi_1 - \varphi_2)\ddot{\varphi}_2 \\ &+R\sin(\varphi_1 - \varphi_2)\dot{\varphi}_2^2 + (m_1 + 2m_2)\ell_1 g \sin(\varphi_1) \\ &-m_2\ell_2 g\sin(\varphi_2) = \tau_1 , \end{aligned} \tag{12}$$

$$\begin{aligned} &R\cos(\varphi_1 - \varphi_2)\ddot{\varphi}_1 + M_2\ddot{\varphi}_2 - R\sin(\varphi_1 - \varphi_2)\dot{\varphi}_1^2 \\ &-m_2\ell_2 g\sin(\varphi_2) = 0 . \end{aligned} \tag{13}$$

The main control objective is to maintain the second arm in a vertical position like an inverted pendulum using the rotation of the (first) actuated arm. In the following, the first arm and the second arm are called *arm* and *pendulum*, respectively. In the physical experiment corresponding to **??** the arm is actuated by a motor driven by a velocity-control power amplifier. The physical quantities are given as follows.

$$\begin{aligned} &\ell_1 = 0.13[m],\ \ell_2 = 0.15[m],\ m_1 = 0.05[kg], \\ &m_2 = 0.03[kg],\ g = 9.8[m/s^2] . \end{aligned} \tag{14}$$

As the velocity $\dot{\varphi}_1$ of the first arm can follow the command input voltage u to the amplifier because of the lightness of the second arm, we can assume that the dynamics from the input voltage to the velocity $\dot{\varphi}_1$ is almost equally given by

$$\frac{d}{dt}\dot{\varphi}_1 = -\frac{1}{T_a}\dot{\varphi}_1 + \frac{K_a}{T_a}u . \tag{15}$$

This means that (12) can be simplified to (15) with reasonable accuracy.

On the other hand, (13) becomes

$$\begin{aligned} &2\ell_1\cos(\varphi_1 - \varphi_2)\ddot{\varphi}_1 + \frac{4}{3}\ell_2\ddot{\varphi}_2 \\ = \quad & g\sin(\varphi_2) + 2\ell_1\sin(\varphi_1 - \varphi_2)\dot{\varphi}_1^2 . \end{aligned} \tag{16}$$

Then, defining

$$r_x := 2\ell_1\sin(\varphi_1) ,\ r_y := 2\ell_1\cos(\varphi_1) , \tag{17}$$

and using (16), another description for the ADIP is as follows :

$$\cos(\varphi_2)\ddot{r}_x + \frac{4}{3}\ell_2\,\ddot{\varphi}_2 = (g + \ddot{r}_y)\sin(\varphi_2) . \tag{18}$$

The pendulum has two kind of equilibrium states:

- unstable equilibrium state: $\varphi_2^* = 0$ (tip pointing upwards)
- stable equilibrium state: $\varphi_2^* = \pi$ (tip pointing downwards)

In this application, we will only consider the difficult situation where the tip is pointing upwards. An immediate linearization of (16) around $\varphi_2^* = 0$ then leads to

$$\ddot{r}_x + \frac{4}{3}\ell_2\,\ddot{\varphi}_2 = (g + \ddot{r}_y)\varphi_2 . \tag{19}$$

Introducing the new variable z defined as

$$z := r_x + \frac{4}{3}\ell_2\varphi_2 , \tag{20}$$

we get

$$\ddot{z} = \frac{3}{4\ell_2}(g + \ddot{r}_y)(z - r_x) . \tag{21}$$

Gathering the equation $\dot{r}_x = r_y\dot{\varphi}_1$ with (15) and (21) the following simple LPV model is obtained

$$\begin{aligned} \frac{d}{dt}\begin{bmatrix} z \\ \dot{z} \\ r_x \\ \dot{\varphi}_1 \end{bmatrix} = \Bigg\{ & \begin{bmatrix} 0 & 1 & 0 & 0 \\ 0 & 0 & 0 & 0 \\ 0 & 0 & 0 & 0 \\ 0 & 0 & 0 & -\frac{1}{T_a} \end{bmatrix} \\ & + \frac{3}{4\ell_2}(g + \ddot{r}_y)\begin{bmatrix} 0 \\ 1 \\ 0 \\ 0 \end{bmatrix}\begin{bmatrix} 1 & 0 & -1 & 0 \end{bmatrix} \\ & + r_y\begin{bmatrix} 0 \\ 0 \\ 1 \\ 0 \end{bmatrix}\begin{bmatrix} 0 & 0 & 0 & 1 \end{bmatrix}\Bigg\}\begin{bmatrix} z \\ \dot{z} \\ r_x \\ \dot{\varphi}_1 \end{bmatrix} \\ & + \begin{bmatrix} 0 \\ 0 \\ 0 \\ \frac{K_a}{T_a} \end{bmatrix} u , \end{aligned} \tag{22}$$

where both z and r_x are assumed to be measured, r_y is viewed as an external time-varying parameters and $\ddot{r}_y$ is assumed to be zero.

In order to derive LPV models with bounds on the time-varying parameters, it is assumed that the arm can rotate within the angular range

$$-\overline{\varphi}_1 \le \varphi_1 \le \overline{\varphi}_1 \quad (0 < \overline{\varphi}_1 < \frac{\pi}{2}) . \tag{23}$$

This yields

$$r_y \in \left[\underline{r_y}, \overline{r_y}\right] := [2\ell_1\cos(\overline{\varphi}_1), 2\ell_1\cos(0)] . \tag{24}$$

From (24), r_y is normalized as

$$\theta_r := \frac{2}{\overline{r_y} - \underline{r_y}}(r_y - \frac{\overline{r_y} + \underline{r_y}}{2}) \in [-1, 1] . \tag{25}$$

Two different though completely equivalent LPV representations can be used for the ADIP. This is described in the sequel.

2.1 LPV model with LFT structure

Representing r_y from (25) as

$$r_y \frac{\overline{r_y} + \underline{r_y}}{2} + \frac{\overline{r_y} - \underline{r_y}}{2}\theta_r$$
$$= \ell_1(1+\cos(\overline{\varphi}_1)) + \ell_1(1-\cos(\overline{\varphi}_1))\theta_r \,, \quad (26)$$

where θ_r denotes the new normalized scheduling variables, the following LPV model of LFT type is obtained.

$$\frac{d}{dt}\begin{bmatrix} z \\ \dot{z} \\ r_x \\ \dot{\varphi}_1 \end{bmatrix} = \begin{bmatrix} 0 & 1 & 0 & 0 \\ \frac{3g}{4\ell_2} & 0 & -\frac{3g}{4\ell_2} & 0 \\ 0 & 0 & 0 & \frac{\overline{r_y}+\underline{r_y}}{2} \\ 0 & 0 & 0 & -\frac{1}{T_a} \end{bmatrix} \begin{bmatrix} z \\ \dot{z} \\ r_x \\ \dot{\varphi}_1 \end{bmatrix}$$
$$+ \begin{bmatrix} 0 \\ 0 \\ \frac{\overline{r_y}-\underline{r_y}}{2} \\ 0 \end{bmatrix} w_r + \begin{bmatrix} 0 \\ 0 \\ 0 \\ \frac{K_a}{T_a} \end{bmatrix} u \,, \quad (27)$$

$$z_r = \begin{bmatrix} 0 & 0 & 0 & 1 \end{bmatrix} \begin{bmatrix} z \\ \dot{z} \\ r_x \\ \dot{\varphi}_1 \end{bmatrix} , \quad (28)$$

with

$$w_r = \theta_r z_r \quad (|\theta_r(t)| \leq 1) \,. \quad (29)$$

2.2 LPV Model with polytopic structure

Similarly, by remarking that

$$\frac{\overline{r_y} - r_y}{\overline{r_y} - \underline{r_y}} + \frac{r_y - \underline{r_y}}{\overline{r_y} - \underline{r_y}} = 1 \,, \quad (30)$$

and introducing the notation

$$\rho_1(r_y) := \frac{\overline{r_y} - r_y}{\overline{r_y} - \underline{r_y}} \,, \; \rho_2(r_y) := \frac{r_y - \underline{r_y}}{\overline{r_y} - \underline{r_y}} \,, \quad (31)$$

we obtain the following LPV polytopic model for the ADIP.

$$\frac{d}{dt}\begin{bmatrix} z \\ \dot{z} \\ r_x \\ \dot{\varphi}_1 \end{bmatrix} = \left(\rho_1(r_y) \begin{bmatrix} 0 & 1 & 0 & 0 \\ \frac{3g}{4\ell_2} & 0 & -\frac{3g}{4\ell_2} & 0 \\ 0 & 0 & 0 & \underline{r_y} \\ 0 & 0 & 0 & -\frac{1}{T_a} \end{bmatrix} \right.$$
$$\left. + \rho_2(r_y) \begin{bmatrix} 0 & 1 & 0 & 0 \\ \frac{3g}{4\ell_2} & 0 & -\frac{3g}{4\ell_2} & 0 \\ 0 & 0 & 0 & \overline{r_y} \\ 0 & 0 & 0 & -\frac{1}{T_a} \end{bmatrix} \right) \begin{bmatrix} z \\ \dot{z} \\ r_x \\ \dot{\varphi}_1 \end{bmatrix}$$
$$+ \begin{bmatrix} 0 \\ 0 \\ 0 \\ \frac{K_a}{T_a} \end{bmatrix} u \,, \quad (32)$$

and it is easily verified that ρ_1 and ρ_2 are polytopic coordinates that is $\rho_1 \geq 0$ and $\rho_2 \geq 0$ and $\rho_1 + \rho_2 = 1$

2.3 Quick look at the wide-range stabilization problem

As already stated in the Introduction, the main control objective for the ADIP is to stabilize the inverted pendulum using the rotations of the arm as depicted in Figure 2 below, and simultaneously increase as much as possible the range where stabilization is achieved. One important difficulty of this problem

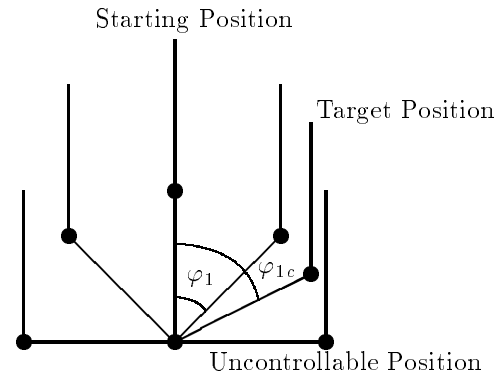

Figure 2: Wide Range Stabilization for the ADIP

comes from the fact that the ADIP becomes uncontrollable as the pendulum gets closer to the horizontal position, hence the need for a gain-scheduled controllers. Apart from the maximation of the range where stabilization holds, we must also provide performance in terms of settling-time and overshoot in response to reference signals. This will be detailed in Section 4. Also the controller should exhibit adequate roll-off in the high-frequency range for noise attenuation.

3 LPV Control Techniques

This section provides a brief review of the design techniques that will be used for the ADIP application. Two LPV design techniques will be investigated hereafter:

- the LFT design technique,
- the polytopic design technique.

As indicated by their names, such techniques apply to LPV plants with LFT and polytopic parameter-dependence, respectively. The first class of LPV plants can be described as

$$\begin{aligned} \dot{x} &= Ax + B_\theta w_\theta + B_1 w + B_2 u \,, \\ z_\theta &= C_\theta x + D_{\theta\theta} w_\theta + D_{\theta 1} w + D_{\theta 2} u \,, \\ z &= C_1 x + D_{1\theta} w_\theta + D_{11} w + D_{12} u \,, \\ y &= C_2 x + D_{2\theta} w_\theta + D_{21} w + D_{22} u \,, \\ w_\theta &= \Theta(t)\, z_\theta \,, \end{aligned} \quad (33)$$

where $\Theta(t)$ is a time-varying parameter matrix and is usually assumed to have a block-diagonal structure in the form

$$\Theta(t) = \mathrm{diag}\,(\ldots, \Theta_i(t), \ldots, \theta_j(t) I, \ldots)\ , \qquad (34)$$

and normalized such that

$$\Theta(t)^T \Theta(t) \leq I, \qquad t \geq 0\,. \qquad (35)$$

Blocks denoted Θ_i and $\theta_j\, I$ are generally referred to as full and repeated-scalar blocks according to the μ analysis and synthesis literature [3, 4]. Note that straightforward computations lead to the state-space representation

$$\begin{bmatrix} \dot{x} \\ z \\ y \end{bmatrix} = \left\{ \begin{bmatrix} A & B_1 & B_2 \\ C_1 & D_{11} & D_{12} \\ C_2 & D_{21} & D_{22} \end{bmatrix} + \begin{bmatrix} B_\theta \\ D_{1\theta} \\ D_{2\theta} \end{bmatrix} \Theta(t) \right.$$
$$\left. \times (I - D_{\theta\theta}\Theta(t))^{-1} \begin{bmatrix} C_\theta & D_{\theta 1} & D_{\theta 2} \end{bmatrix} \right\} \begin{bmatrix} x \\ w \\ u \end{bmatrix}\ , \qquad (36)$$

hence the plant with inputs w and u and outputs z and y has state-space data entries which are fractional functions of the time-varying parameter $\Theta(t)$. Hereafter, we are using the following notation

- u for the control signal
- w for exogenous inputs
- z for controlled or performance variables
- y for the measurement signal.

As an alternative to this description, we are also considering polytopic systems which are described by the state-space representation

$$\begin{aligned} \dot{x} &= A(\rho(t))x + B_1(\rho(t))w + B_2(\rho(t))u\,, \\ z &= C_1(\rho(t))x + D_{11}(\rho(t))w + D_{12}(\rho(t))u\,, \\ y &= C_2(\rho(t))x + D_{21}(\rho(t))w + D_{22}(\rho(t))u\,, \end{aligned} \qquad (37)$$

where generally, $A(\rho)$, $B_1(\rho)$, ... are affine functions of the time-varying parameter $\rho(t)$ evolving in a polytopic set $\mathcal{P}_\rho$, i.e.,

$$\rho(t) \in \mathcal{P}_\rho := \mathrm{co}\,\{\rho_{v_1}, \ldots, \rho_{v_r}\}\,, \qquad t \geq 0, \qquad (38)$$

where the notation co $\{.\}$ stands for the convex hull of the set $\{.\}$.

Clearly, the state-space data of the plant (37) range over a matrix polytope and thus it trivially holds that

$$\begin{bmatrix} A(\rho(t)) & B_1(\rho(t)) & B_2(\rho(t)) \\ C_1(\rho(t)) & D_{11}(\rho(t)) & D_{12}(\rho(t)) \\ C_2(\rho(t)) & D_{21}(\rho(t)) & D_{22}(\rho(t)) \end{bmatrix} \in$$
$$\mathcal{P} := \mathrm{co}\left\{ \begin{bmatrix} A_i & B_{1i} & B_{2i} \\ C_{1i} & D_{11i} & D_{12i} \\ C_{2i} & D_{21i} & D_{22i} \end{bmatrix},\ i = 1, 2, \ldots, r \right\}\ , \qquad (39)$$

where

$$\begin{aligned} & \begin{bmatrix} A_i & B_{1i} & B_{2i} \\ C_{1i} & D_{11i} & D_{12i} \\ C_{2i} & D_{21i} & D_{22i} \end{bmatrix} \\ := & \begin{bmatrix} A(\rho_{v_i}) & B_1(\rho_{v_i}) & B_2(\rho_{v_i}) \\ C_1(\rho_{v_i}) & D_{11}(\rho_{v_i}) & D_{12}(\rho_{v_i}) \\ C_2(\rho_{v_i}) & D_{21}(\rho_{v_i}) & D_{22}(\rho_{v_i}) \end{bmatrix}, \\ & i = 1, \ldots, r\,. \end{aligned} \qquad (40)$$

For any of the LPV plants (33)-(35) or (37)-(39), the LPV control problem (often referred to as the gain-scheduling control problem) consists in seeking an LPV controller

$$\begin{aligned} \dot{x}_K &= A_K(p)x_K + B_K(p)y\,, \\ u &= C_K(p)x_K + D_K(p)y\,, \end{aligned} \qquad (41)$$

where $p(t) = \Theta(t)$ for the LFT-LPV plant (33)-(35) and $p(t) = \rho(t)$ for the polytopic LPV plant (37)-(39) such that

- the closed-loop system (33)-(35) and (41) or the closed-loop system (37)-(39) and (41) is internally stable,
- the L_2-induced gain of the operator connecting w to z is bounded by γ,

for all parameter trajectories $p(t)$ defined by either (35) or (39).

It is now well-known that such problems can be handled via a suitable generalization of the Bounded Real Lemma. The following LMI characterizations for the solvability of such problems is then obtained. The reader is referred to references [5, 6, 7, 8, 13, 12] for more details and additional results.

3.1 Solvability conditions for LFT plants

The characterization of the solutions to the LPV control problem for LFT plants requires the definitions of scaling sets compatible with the parameter structure given in (34). Denoting this structure as $\mathbf{\Theta}$, the following scaling sets can be introduced. The set of symmetric scalings associated with the parameter structure $\mathbf{\Theta}$ is defined as

$$S_{\mathbf{\Theta}} := \{S : S^T = S, \quad S\Theta = \Theta S,$$
$$\forall \Theta \text{ with structure } \mathbf{\Theta}\}\ .$$

Similarly, the set of skew-symmetric scalings associated with the parameter structure $\mathbf{\Theta}$ is defined as

$$T_{\mathbf{\Theta}} := \{T : T^T = -T, \quad T\Theta = \Theta^T T,$$
$$\forall \Theta \text{ with structure } \mathbf{\Theta}\}\ .$$

Equivalently, it is easily verified that with $S > 0$, the scheduled matrix Θ satifies the quadratic constraints in

$$\begin{bmatrix} I \\ \Theta \end{bmatrix}^T \begin{bmatrix} S & T \\ T^T & -S \end{bmatrix} \begin{bmatrix} I \\ \Theta \end{bmatrix} \geq 0,$$

$$\forall \Theta \text{ s. t. } \Theta^T \Theta \leq I, \quad \text{with structure } \mathbf{\Theta}.$$

With the above definitions and notations in mind, the following LMI characterization for the solvability of the problem can be established.

Theorem 3.1 *Consider the LFT plant governed by (33) and (35) with Θ assuming a block-diagonal structure as in (34). Let $\mathcal{N}_X$ and $\mathcal{N}_Y$ denote any bases of the null spaces of $[C_2, D_{2\theta}, D_{21}, 0]$ and $[B_2^T, D_{\theta 2}^T, D_{12}^T, 0]$, respectively. Then, there exists an LPV controller such that the (scaled) Bounded Real Lemma conditions hold for some guaranteed L_2-performance level γ if and only if there exist pairs of symmetric matrices (X, Y), (S_3, Σ_3) and a pair of skew-symmetric matrices (T_3, Γ_3) such that the structural constraints*

$$S_3,\ \Sigma_3 \in S_{\mathbf{\Theta}} \text{ and } T_3,\ \Gamma_3 \in T_{\mathbf{\Theta}} \tag{42}$$

hold, and the LMIs

$$\mathcal{N}_X^T \begin{bmatrix} A^T X + XA & XB_\theta + C_\theta^T T_3^T & XB_1 & C_\theta^T S_3 & C_1^T \\ B_\theta^T X + T_3 C_\theta & -S_3 + T_3 D_{\theta\theta} + D_{\theta\theta}^T T_3^T & T_3 D_{\theta 1} & D_{\theta\theta}^T S_3 & D_{1\theta}^T \\ B_1^T X & D_{\theta 1}^T T_3^T & -\gamma I & D_{\theta 1}^T S_3 & D_{11}^T \\ S_3 C_\theta & S_3 D_{\theta\theta} & S_3 D_{\theta 1} & -S_3 & 0 \\ C_1 & D_{1\theta} & D_{11} & 0 & -\gamma I \end{bmatrix} \mathcal{N}_X < 0\,, \tag{43}$$

$$\mathcal{N}_Y^T \begin{bmatrix} AY + YA^T & YC_\theta^T + B_\theta \Gamma_3^T & YC_1^T & B_\theta \Sigma_3 & B_1 \\ C_\theta Y + \Gamma_3 B_\theta^T & -\Sigma_3 + \Gamma_3 D_{\theta\theta}^T + D_{\theta\theta} \Gamma_3^T & \Gamma_3 D_{1\theta}^T & D_{\theta\theta} \Sigma_3^T & D_{\theta 1} \\ C_1 Y & D_{1\theta} \Gamma_3^T & -\gamma I & D_{1\theta} \Sigma_3 & D_{11} \\ \Sigma_3 B_\theta^T & \Sigma_3 D_{\theta\theta}^T & \Sigma_3 D_{1\theta}^T & -\Sigma_3 & 0 \\ B_1^T & D_{\theta 1}^T & D_{11}^T & 0 & -\gamma I \end{bmatrix} \mathcal{N}_Y < 0\,, \tag{44}$$

$$\begin{bmatrix} X & I \\ I & Y \end{bmatrix} > 0\,, \tag{45}$$

$$\begin{bmatrix} S_3 & 0 \\ 0 & \Sigma_3 \end{bmatrix} > 0 \tag{46}$$

are feasible.

Remark 3.2 The characterization given in Theorem 3.1 constitutes a standard semi-definite program, that is, minimize the linear objective γ subject to the LMI constraints (43)-(46), and can be solved with very efficient interior-point techniques as in [14, 15, 16, 17].

3.2 Solvability conditions for polytopic plants

A similar characterization can be derived for polytopic LPV plants by invoking a suitable extension of the Bounded Real Lemma [5, 8].

For simplicity, it is first assumed that $B_2(\rho)$, $C_2(\rho)$, $D_{12}(\rho)$, $D_{21}(\rho)$ are parameter-independent or equivalently,

$$\begin{bmatrix} B_{2i} \\ D_{12i} \end{bmatrix} = \begin{bmatrix} B_2 \\ D_{12} \end{bmatrix}, \quad [\, C_{2i} \quad D_{21i} \,] = [\, C_2 \quad D_{21} \,], \quad i = 1, 2, \ldots, r. \tag{47}$$

Theorem 3.3 *Consider the polytopic plant (37) and (39) and let $\mathcal{N}_X$ and $\mathcal{N}_Y$ denote bases of the null spaces of $[\, C_2, D_{21}, 0 \,]$ and $[\, B_2^T, D_{12}^T, 0 \,]$, respectively. Then, there exists an LPV controller such that the (extended) Bounded Real Lemma conditions hold in closed-loop for some L_2-performance level γ if and only if there exist a pair of symmetric matrices (X, Y) satisfying the LMI conditions:*

$$\mathcal{N}_X^T \begin{bmatrix} A_i^T X + XA_i & XB_{1i} & C_{1i}^T \\ B_{1i}^T X & -\gamma I & D_{11i}^T \\ C_{1i} & D_{11i} & -\gamma I \end{bmatrix} \mathcal{N}_X < 0\,, \tag{48}$$

$$\mathcal{N}_Y^T \begin{bmatrix} A_i Y + YA_i^T & YC_{1i}^T & B_{1i} \\ C_{1i} Y & -\gamma I & D_{11i} \\ B_{1i}^T & D_{11i}^T & -\gamma I \end{bmatrix} \mathcal{N}_Y < 0\,, \tag{49}$$

$$\begin{bmatrix} X & I \\ I & Y \end{bmatrix} > 0 \tag{50}$$

for $i = 1, \ldots, r$.

Using a slightly different approach, it is possible to characterize multiple and multi-channel specifications in the case of polytopic LPV systems [10, 19, 9]. Since it has proved useful in the ADIP control, we briefly introduce the LMIs characterizing L_2-gain performance in conjunction to LMI region constraints on the pole of the closed-loop system. The reader is referred to [19, 20] for a thorough discussion on LMI regions and their use in robust control theory. For completeness, we must mention that LMI regions of the complex plane are very general. As examples, vertical and horizontal strips, circles, conic sectors, ... and intersections of such regions are LMI regions. Moreover, any self-conjugate region of the complex plane can be aproximated to any desired accuracy with an LMI region. LMI region are more formally characterized as the set

$$\left\{ z \in \mathbf{C} : \, L + zM + \bar{z} M^T < 0 \right\}. \tag{51}$$

For the polytopic system (37), it is not difficult to establish the following [9].

Theorem 3.4 *There exists an LPV controller such that*

- *the (extended) Bounded Real Lemma conditions hold in closed-loop for some L_2-performance level γ,*
- *at frozen (with respect to time) values of the parameter ρ the closed-loop system has all its poles in the LMI region (51)*

whenever there exist symmetric matrices Y and X and quadruples $(\widehat{A}_{K,i}, \widehat{B}_{K,i}, \widehat{C}_{K,i}, \widehat{D}_{K,i})$ such that the following LMI problem is feasible,

$$\begin{bmatrix} XA_i + \widehat{B}_{K,i}C_2 + (\star) & * & \star & \star \\ \widehat{A}_{K,i}^T + A_i + B_2\widehat{D}_{K,i}C_2 & A_iY + B_2\widehat{C}_{K,i} + (\star) & \star & \star \\ (XB_{1i} + \widehat{B}_{K,i}D_{21})^T & (B_{1i} + B_2\widehat{D}_{K,i}D_{21})^T & -\gamma I & \star \\ C_{1i} + D_{12}\widehat{D}_{K,i}C_2 & C_{1i}Y + D_{12}\widehat{C}_{K,i} & D_{11i} + D_{12}\widehat{D}_{K,i}D_{21} & -\gamma I \end{bmatrix} < 0\,, \tag{52}$$

$$\left(L_{jk}\begin{bmatrix} Y & I \\ I & X \end{bmatrix} + M_{jk}\begin{bmatrix} A_iY + B_2\widehat{C}_{K,i} & A_i + B_2\widehat{D}_{K,i}C_2 \\ \widehat{A}_{K,i} & XA_i + \widehat{B}_{K,i}C_2 \end{bmatrix} + M_{kj}[\star]^T \right)_{j,k} < 0\,, \tag{53}$$

$$\begin{bmatrix} X & I \\ I & Y \end{bmatrix} > 0 \tag{54}$$

for i=1,...,r.

Remark 3.5 As before the conditions given in Theorems 3.3 and 3.4 not only secure stability and performance for any admissible frozen value of the parameter ρ but also for any time-dependent trajectory $\rho(t)$ confined to (38). However, the additional LMI region pole constraint in Theorem 3.4 only makes sense at frozen values of ρ in its polytopic range.

When solutions to the LMI conditions of Theorems 3.1 or 3.3 have been found, the state-space data of the controller in (41) can be computed for any admissible value of the parameter $\Theta(t)$ or $p(t)$, using well-known schemes. The reader is referred to [18, 21] and [7, 8, 9] for a comprehensive discussion.

4 LPV Controller Synthesis for the ADIP

In this section, we first give a thorough description of the specifications and control objectives together with the control structure used for the ADIP. Next different robust and LPV syntheses are carried out and results are discussed with regards to the specifications introduced earlier but also from the viewpoint of the ease of implementation on the physical experiment. This last phase has revealed necessary since we have found some mismatches between computerized nonlinear simulations and the 'real' responses on the ADIP.

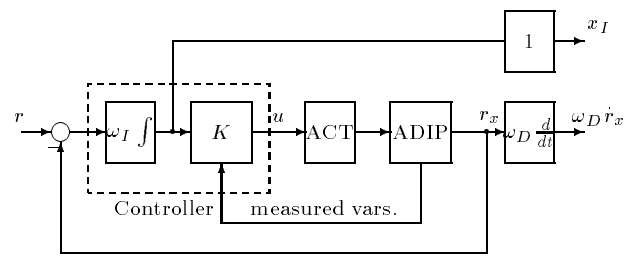

Figure 3: Interconnection Structure for the ADIP

4.1 Problem presentation and specifications

For the designs, we shall be using the synthesis interconnection shown in Figure 3. The serial connection of the ADIP and the actuator (ACT) is described by (27)-(29) or (31)-(32) depending on the particular LPV representation we are actually using. Note that we have introduced some integral action in the forward channel to ensure zero steady-state tracking error at an equilibrium position. The integral action is here described as

$$\dot{x}_I = \omega_I(r - r_x)\,, \tag{55}$$

where ω_I is a design parameter. The family of test or reference signals r for the arm rotation in the range (23) which are used hereafter can be described as follows.

$$r(t) := \begin{cases} \frac{r_{max}}{\tau}t & (0 \le t \le \tau) \\ r_{max} & (\tau \le t \le \frac{T}{2} - \tau) \\ -\frac{r_{max}}{\tau}(t - \frac{T}{2}) & (\frac{T}{2} - \tau \le t \le \frac{T}{2} + \tau) \\ -r_{max} & (\frac{T}{2} + \tau < t < T - \tau) \\ \frac{r_{max}}{\tau}(t - T) & (T - \tau \le t \le T) \end{cases} \tag{56}$$

where $r_{max} := 2\ell_1 \cos(\varphi_{1c})$, $\tau = 0.5$ and $\varphi_{1c}(\le \overline{\varphi}_1)$ is a target value. A simple drawing of such signals is depicted in Figure 4. Then the specifications for the control system are the following:

(S1) the closed-loop system is internally stable.

(S2) the L_2-induced gain of the operator connecting $w = r$ to $z = \begin{bmatrix} \omega_D \dot{r}_x \\ x_I \end{bmatrix}$ is bounded by γ, where ω_D is a design parameter.

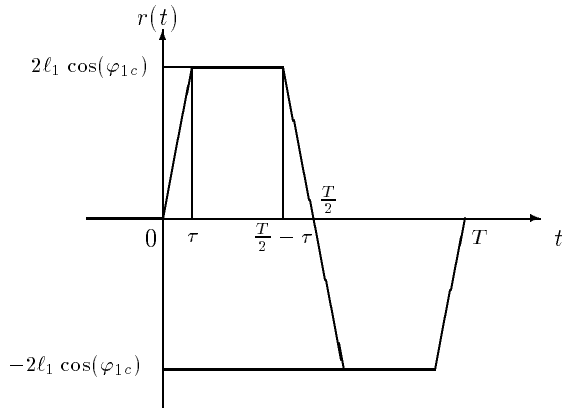

Figure 4: The Command $r(t)$

(S3) specifications **(S1)** and **(S2)** must hold on the largest range of $\overline{\varphi}_1$ as far as possible.

(S4) the LPV controller must be implementable with a minimum sampling interval 2.5[msec].

The specification **(S1)** means that the LPV controller must stabilize the inverted pendulum in any vertical position in the range $\varphi_1 \in [-\overline{\varphi}_1, \overline{\varphi}_1]$. Besides, the specification **(S2)** translates performance tracking and high-frequency gain attenuation objectives. The specification **(S3)** express that stabilization but also performance and roll-off requirements must be achieved on the largest range of possible dynamics of the ADIP. The specification **(S4)** is directly dictated from physical hardware limitations.

4.2 Robust LTI syntheses

Before utilizing the LPV synthesis techniques introduced in in Section 3, it is instructive to investigate what can be achieved using customary robust control techniques such as H_∞ and μ syntheses. Note first that since the synthesis problem depicted in Figure 3 is completely singular ($D_{12} = 0$ and $D_{21} = 0$), any H_∞ synthesis steps were performed using the LMI formulation in [18], which is not restricted by singularity problems. Moreover, in order to satisfy the implementation constraints **(S4)**, which require reasonable controller dynamics, we also have introduced LMI region pole constraints on the closed-loop dynamics. This requires using the refined H_∞ synthesis technique in [19] (See also Section 3). The LMI region under consideration is determined by the intersection of a half-plane, a conic sector and a disk as shown in Figure 5.

4.2.1 H_∞ synthesis based on a nominal model

Based on a nominal model (ADIP in vertical position $\varphi_1 = 0$, i.e. $\overline{\varphi}_1 = 0$), an H_∞ controller has been

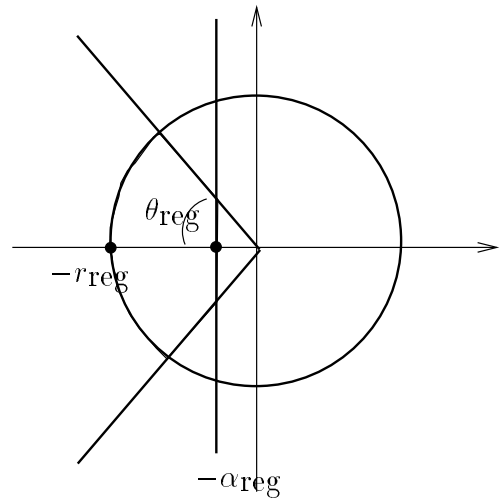

Figure 5: LMI region for the closed-loop system

computed leading to a performance level $\gamma = 2.5774$ where the $\omega_D = 0.02, \omega_I = 0.5$ and the LMI region constraint is determined by $\alpha_{reg} = 0.5, r_{reg} = 50, \theta_{reg} = 45°$. The poles of the H_∞ controller are given as

$$\{-67.166,\ -49.834 \pm 19.109j,\ -39.3169,\ -0.1319,\ 0\}\,.$$

Note that this is in stark contrast with the result obtained without pole constraints which yielded the controller poles

$$\{-3.3110 \times 10^5,\ -5.8209 \times 10^4,\ -3.97759 \times 10^4,\ -2.0037 \times 10^4,\ -22.806,\ 0\}\,.$$

Such dynamics clearly do not satisfy the implementation constraints **(S4)** and thus must be ruled out in this application. So, we only retained the first H_∞ controller. The corresponding nonlinear simulations using the realistic model (3) are compared with records on the "true" experiment in Figure 6. For each figure, the (1,1)-subplot shows the command r and the time-response of φ_1, the (1,2)-subplot shows φ_2, the (2,1)-subplot shows the control signal u, and the (2,2)-subplot shows θ_r. We first observe the consistency of the responses of the simulation and the experiment, which to some extent validates the simplified model we have used for synthesis. One can also see that the control system has very poor performance using this controller even on the somewhat reduced target $\varphi_{1c} = 45°$.

4.2.2 μ controller based on an uncertain model

We decided to improve these preliminary results using μ synthesis by explicitly taking account of the

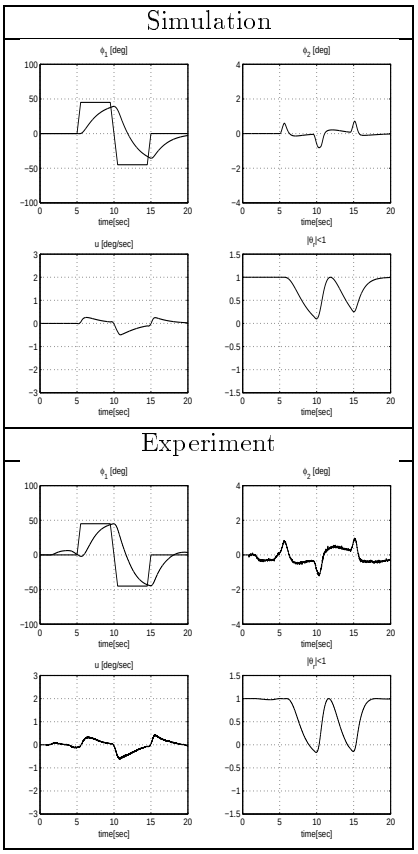

Figure 6: H_∞ control system ($\gamma = 2.5774$, $\varphi_{1c} = 45°$)

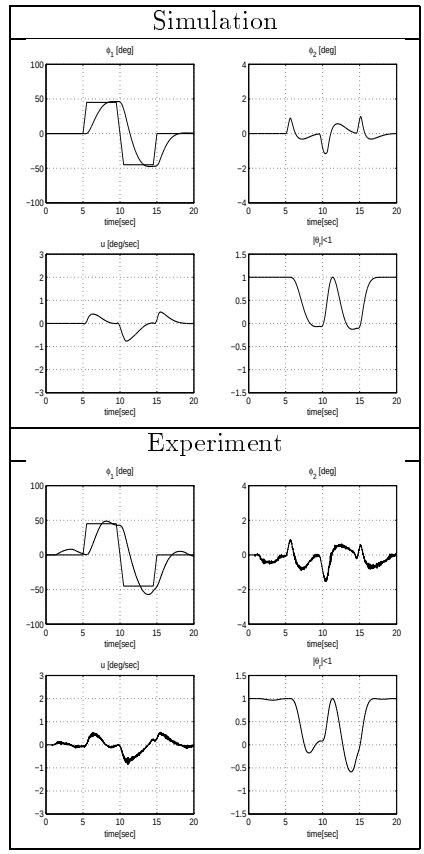

Figure 7: μ control system ($\gamma = 0.7938$, $\varphi_{1c} = 45°$)

changing dynamics of the ADIP, where $\overline{\varphi}_1 = 65°$. Using first-order μ scaling and the parameters tuned to $\omega_D = 0.02, \omega_I = 0.8$ and $\alpha_{reg} = 0.1, r_{reg} = 50, \theta_{reg} = 45°$, we converged using the μ-Analysis and Synthesis Toolbox (with the H_∞ synthesis steps enforcing closed-loop pole constraints) to some controller with poles

$$\{-61.497 \pm 25.596j,\ -47.080,\ -33.753,\\ -0.8993,\ -0.3723,\ -0.2206,\ 0\},$$

which are clearly satisfactory with respect to the implementation constraints. In our example, usual μ synthesis algorithms would lead to unacceptable controller dynamics. As before, the nonlinear simulations and the hardware experiment are shown in Figure 7.

As expected, this second controller provides better performance on the target $\varphi_{1c} = 45°$. However, the very same controller but with the target φ_{1c} increased to 60° does not even provide stability and we did not find any simple way to guarantee the same level of performance on this larger range.

Summing up our results, the H_∞ controller is able to stabilize the range 45° but provides very poor performance. The μ controller provides adequate performance on the range 45° but does not longer work for ranges up to 60° hence illustrating a fundamental tradeoff between performance and the size of the operating range. In many applications this tradeoff is very limiting and can only be negotiated outside the set of fixed controller structures by exploiting gain-scheduling strategies. This is considered in the next section.

4.3 LPV syntheses

In this section, the synthesis techniques discussed in Section 3 are exploited to improve both performance and the operating range of the ADIP.

4.3.1 Design of a LFT controller

An LFT controller is designed using the LFT description of the ADIP, where $\overline{\varphi}_1 = 65°$. The parameters ω_D and ω_I were set to 0.02 and 0.5, respectively. The underlying LTI dynamics of the LFT controller are easily obtained by instantiating the LFT controller at some frozen values of θ_r. For the extreme values of θ_r the following dynamics are obtained.

$$\theta_r = 1 : \{-365.56,\ -359.74,\ -291.81,\ -24.064,\\ -1.3786,\ 0\},$$

$$\theta_r = -1 : \{-365.56,\ -359.72,\ -291.84,\ -42.888,$$

$$-1.4367,\ 0\}\,.$$

Such dynamics are again satisfactory in regards to implementation constraints and have been derived by minimizing, through an LMI formulation, the norm of the A matrix of the LPV controller in the construction procedure. The nonlinear simulations and the hardware experiments are shown in Figure 8. As expected, both performance and the the size of the operating range have been enhanced as compared to previous LTI controllers.

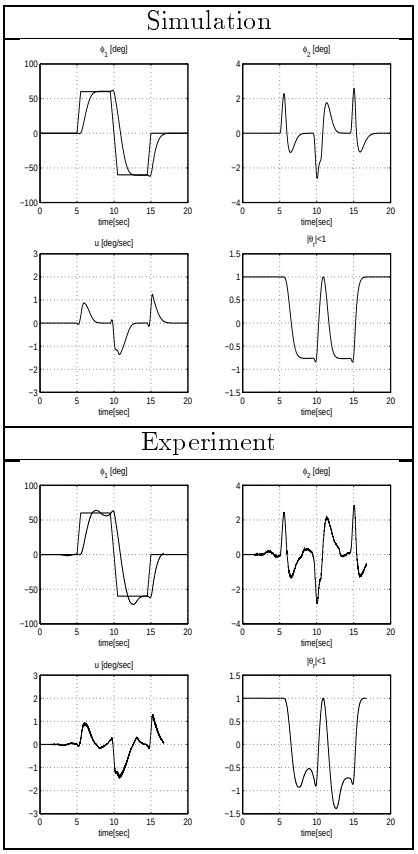

Figure 8: LFT control system ($\gamma = 0.4733$, $\varphi_{1c} = 60°$)

4.3.2 Design of a polytopic controller

A similar design is now conducted using the polytopic description of the ADIP, where $\overline{\varphi}_1 = 65°$, hence leading to polytopic LPV controllers. In order to satisfy the implementation constraints **(S4)**, we have used the refined synthesis technique of Theorem 3.4 which can handle constraints on the closed-loop dynamics. With the selection $\omega_D = 0.1, \omega_I = 0.5$ and $\alpha_{reg} = 1, r_{reg} = 50, \theta_{reg} = 45°$, the underlying LTI controllers obtained at the extreme values of the parameter range have the following dynamics

$$\varphi_1 = 0° : \{-69.352 \pm 50.251j,\ -53.529,\ -20.775,\ -3.6379,\ 0\}\,,$$

$$\varphi_1 = 65° : \{-76.0805,\ -35.506 \pm 41.303j,\ -35.159,\ -2.1349,\ 0\}\,.$$

They are again satisfactory. The nonlinear simulations and the hardware experiments with the polytopic controller are shown in Figure 9. It is again observed that again very good performance is achieved over the same operating range.

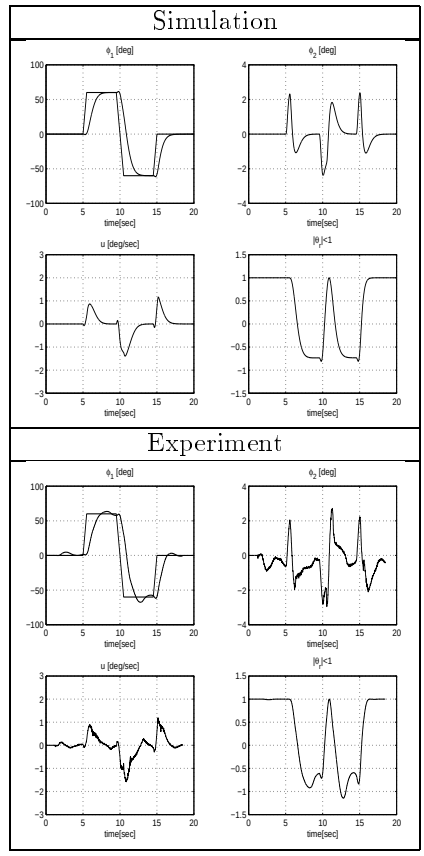

Figure 9: Polytopic control system ($\gamma = 0.4729$, $\varphi_{1c} = 60°$)

4.4 LPV Controller Implementation

For completeness, we give a brief description of the implementation of LPV controllers both for the nonlinear simulations and for the experiments. Note first that due to their inherent time-varying nature, LPV controllers are generally harder to implement than classical LTI controllers. It is shown below that nonlinear simulations can be easily performed using SIMULINK, and that LPV controllers can be implemented on the ADIP with little effort using the REAL-TIME WORKSHOP.

In order to perform the controller implementations, we have used the flexibility offered by SIMULINK which only requires the construction of dynamic blocks together with their interconnections. For the nonlinear simulations of the closed-loop systems involving the LFT controllers, we used the

block-diagram as shown in the left-hand side of Figure 10. It consists of the following principal blocks.

- `ADIP`: the nonlinear simulator block of ADIP based on (15)-(16)
- `PP`: the pre-processing block is computing relevant outputs consisting of the scheduled variable θ_r by (25), the measurement $r_x = 2\ell_1 \sin(\varphi_1)$, and the measurement $z - r_x = \frac{4\ell_2}{3}\varphi_2$. These variables are calculated from the values of φ_1 and φ_2 detected by two encoders.
- `LTISS`: this block corresponds to the LTI part of the LFT controllers and can be detailed as follows.

$$\begin{aligned} \dot{x}_c &= A_c x_c + B_c y_c \,, \\ u_c &= C_c x_c + D_c y_c \,, \end{aligned} \tag{57}$$

with $y_c = \begin{bmatrix} r_x \\ \frac{4\ell_2}{3}\varphi_2 \\ r \\ w_r \end{bmatrix}$, $u_c = \begin{bmatrix} u \\ z_r \end{bmatrix}$, and the feedback relation $w_r = \theta_r z_r$.

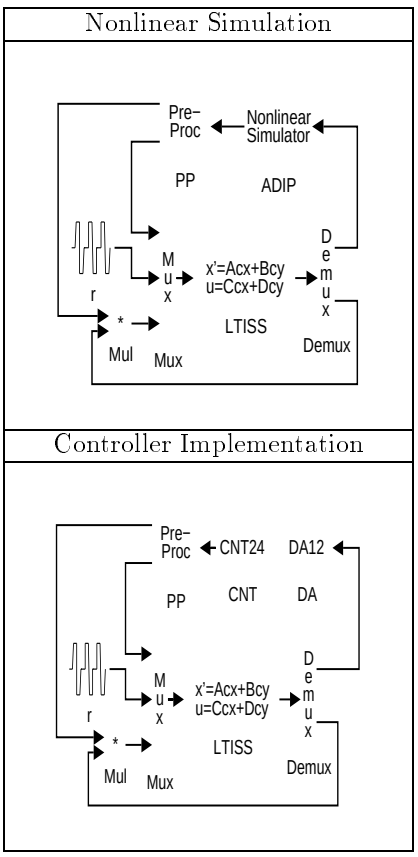

Figure 10: LFT controller

Similarly, as shown in the right-hand side of the figure, the LFT structure is also easily implemented on the (physical) ADIP by replacing the nonlinear simulator block `ADIP` with the I/O driver blocks `CNT` and `DA`. Then it becomes fairly straightforward to generate the C code associated with the LFT controller. This C code is then linked to a Runge-Kutta solver using the facilities of the REAL-TIME WORKSHOP to constitute the discrete-time LPV controller. Note that the designer completely avoids the discretization phase in such a procedure.

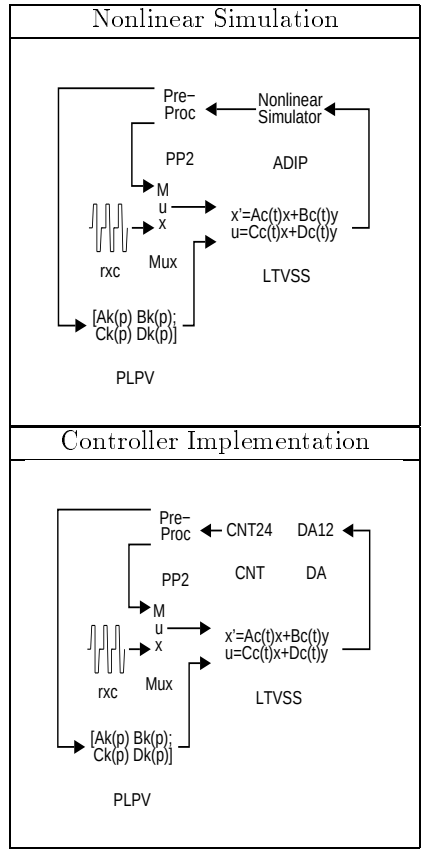

Figure 11: Polytopic controller

For polytopic LPV controllers, the relevant diagrams are those of Figure 11. In addition to `ADIP` and `PP` with the scheduled variable r_x by (17), we have the following new blocks.

- `LTVSS`: the solver block of the differential equation related to a general linear time-varying (LTV) system

$$\begin{aligned} \dot{x}_c &= A_c(t) x_c + B_c(t) y_c \,, \\ u_c &= C_c(t) x_c + D_c(t) y_c \,, \end{aligned} \tag{58}$$

where $y_c = \begin{bmatrix} r_x \\ \frac{4\ell_2}{3}\varphi_2 \\ r \end{bmatrix}$, $u_c = u$.

- `PLPV`: this block is only for computing the state-space data of the polytopic controller at the current value of the scheduled variable $r_y(t)$, we have

$$\begin{bmatrix} A_K(\rho(t)) & B_K(\rho(t)) \\ C_K(\rho(t)) & D_K(\rho(t)) \end{bmatrix}$$

$$= \underbrace{\frac{\overline{r_y} - r_x(t)}{\overline{r_y} - \underline{r_y}}}_{\rho_1(t)} \underbrace{\begin{bmatrix} A_{K1} & B_{K1} \\ C_{K1} & D_{K1} \end{bmatrix}}_{S_{K1}}$$

$$+ \underbrace{\frac{r_x(t) - \underline{r_y}}{\overline{r_y} - \underline{r_y}}}_{\rho_2(t)} \underbrace{\begin{bmatrix} A_{K2} & B_{K2} \\ C_{K2} & D_{K2} \end{bmatrix}}_{S_{K2}} . \qquad (59)$$

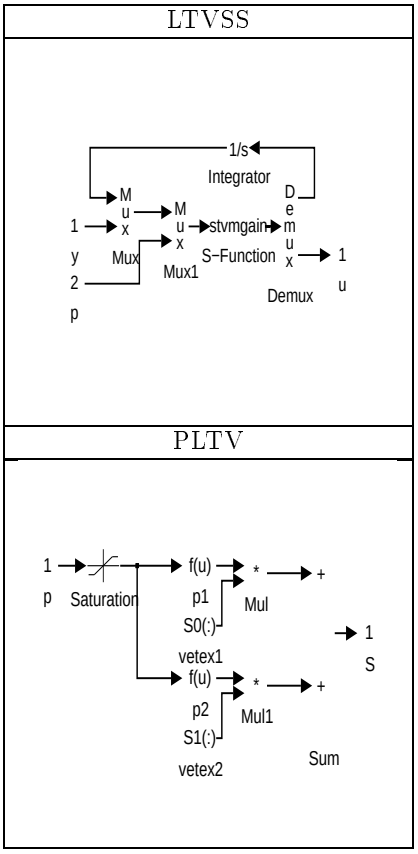

Figure 12: LTVSS and PLTV

The inside of the blocks `LTVSS` and `PLPV` is detailed in Figure 12. The block `LTVSS` is simply the time-varying version of the `LTISS` block. The `S-function` block called `stvmgain` is simply computing the matrix-vector products in the right-hand sides of (58) and the LTV system (58) is represented by an upper LFT in the form

$$\begin{bmatrix} \dot{x}_c \\ u_c \end{bmatrix} = \mathcal{F}_u \left(\begin{bmatrix} A_c(t) & B_c(t) \\ C_c(t) & D_c(t) \end{bmatrix}, \frac{1}{s} \right) \begin{bmatrix} x_c \\ y_c \end{bmatrix} . \quad (60)$$

The `PLTV` block is computing the state-space data using (59), which are then provided to the `LTVSS` block in vectorized form.

5 Concluding Remarks

We can summarize the results of the four kinds of synthesis methods as shown in Table 1.

synthesis	γ	$\overline{\varphi}_1$	φ_{1c}	T_s
H_∞	2.57	-	45°	5s
μ	0.79	65°	45°	2.5s
LFT-LPV	0.47	65°	60°	2s
Poly-LPV	0.42	65°	60°	2s

Table 1: Performance indeces for LTI and LPV methods

This shows that each synthesis method can theoretically stabilize the operating range $[-\overline{\varphi}_1, \overline{\varphi}_1]$ but experimentally dose $[-\varphi_{1c}, \varphi_{1c}]$. As for the μ-synthesis, we observe some gap between the two range, that is, $\overline{\varphi}_1 = 65°$ and $\varphi_{1c} = 45°$. This may come from the fact that we adopted the approximated mathematical model for thr ADIP. In Table 1, T_s indicates the settlinig time in the experiments.

We can address the important comments about the LTI and LPV methods as shown in Table 2.

synthesis	comments
H_∞	less performance needs pole constraint
μ	often higher order needs pole constraint
LFT-LPV	no direct pole constraint treats general dependence
Poly-LPV	pole constraint OK treats only affine dependence

Table 2: Merits and demerits in LTI and LPV methods

We have presented a comprehensive application of LPV control techniques to the control of an arm-driven inverted pendulum. The particular interest of this application lies in the fact that all ingredients of the design problem have to be taken into account, from the specifications up to the constraints inherent to real-world implementations. In this context, it has been shown that currently available synthesis methodologies such as μ and LPV techniques may fail to provide acceptable answers. A major obstacle is undoubtly the implementation constraint that puts hard limitations on the controller dynamics. These limitations are generally difficult to handle within the usual formulation of LPV control techniques. It has been shown that a suitable extension of these techniques including LMI region contraints on the closed-loop dynamics allows to overcome this difficulty. When implementable, it has been observed that LPV controllers outperform fixed μ controllers both in robustness and performance. These observations were confirmed by simulations but more importantly by a number of records on the physical experiment.

References

[1] M. W. Spong and M. Vidyasagar: Robot Dynamics and Control, Wiley, 1989

[2] C. Canudas de Wit, B. Siciliano and G.Bastin (eds.): The Theory of Robot Control, Springer, 1996

[3] M. K. H. Fan, A. L. Tits and J. C. Doyle: Robustness in the Presence of Mixed Parametric Uncertainty and Unmodelized Dynamics, *IEEE Trans. Automat. Contr.*, vol.AC-36, no.1, pp.25-38

[4] J. C. Doyle and A. Packard and K. Zhou: Review of LFT's, LMI's and μ, *CDC Brighton, England*, pp.1227-1232, 1991

[5] A. Packard and G. Becker: Quadratic Stabilization of Parametrically-Dependent Linear Systems using Parametrically-Dependent Linear, Dynamic Feedback, *Advances in Robust and Nonlinear Control Systems*, vol.DSC-43, pp.29-36, 1992

[6] A. Packard: Gain Scheduling via Linear Fractional Transformations, *Syst. Contr. Lett.*, vol.22, no.2, pp.79-92, 1994

[7] P. Apkarian and P. Gahinet: A Convex Characterization of Gain-Scheduled H_∞ Controllers, *IEEE Trans. Automat. Contr.*, vol.40, no.5, pp.853-864, 1995

[8] P. Apkarian, P. Gahinet, G. Becker: Self-Scheduled H_∞ Control of Linear Parameter-Varying Systems: A Design Example, *Automatica*, vol.31, no.9 pp.1251-1261, 1995

[9] P. Apkarian, R. J. Adams: Advanced Gain-Scheduling Techniques for Uncertain Systems, *IEEE Trans. on Control System Technology*, to appear, 1998

[10] C. Scherer: Mixed H_2/H_∞ Control, *Trends in Control: A European Perspective*, volume of the Special Contribution to the ECC 95

[11] C. Scherer: Mixed H_2/H_∞ Control for Linear Parametrically Varying Systems, *CDC New Orleans, LA*, pp. 3182-3187, 1995

[12] G. Scorletti and L. El. Ghaoui: Improved Linear Matrix Inequality Conditions for Gain-Scheduling, *CDC New Orleans, LA*, pp.3626-3631, 1995

[13] A. Helmersson: Methods for Robust Gain-Scheduling, Ph. D. Thesis, Linkoping University, Sweden, 1995

[14] Yu. E. Nesterov and A. S. Nemirovski: Interior Point Polynomial Methods in Convex Programming: Theory and Applications, SIAM Studies in Applied Mathematics vol.13, SIAM, 1994

[15] L. Vanderberghe and S. Boyd: Primal-Dual Potential Reduction Method for Problems Involving Matrix Inequalities, *Math. Programming Series B*, no.69, pp.205-236, 1995

[16] S. Boyd and L. El. Ghaoui: Method of Centers for Minimizing Generalized Eigenvalues, *Lin. Alg. and Applic.*, vol.188, pp.63-111, 1992

[17] P. Gahinet and A. Nemirovski: General-Purpose LMI Solvers with Benchmarks, *CDC San Antonio*, pp.3162-3165, 1993

[18] P. Gahinet and P. Apkarian: A Linear Matrix Inequality Approach to H_∞ Control, *Int. J. Robust and Nonlinear Contr.*, vol.4, pp.421-448, 1994

[19] M. Chilali and P. Gahinet: H_∞ Design with Pole Placement Constraints: an LMI Approach, *IEEE Trans. Autom. Contrl.*, vol. 41, 3, pp. 358-367, 1996

[20] G. Garcia and D. Arzelier and J. Daafouz and J. Bernussou: An LMI Formulation for Robust Disk Pole Assignment via Output Feedback, *IFAC World Congress*, San Fransisco, 1996

[21] T. Iwasaki and R. E. Skelton: All Controllers for the General H_∞ Control Problem: LMI Existence Conditions and State Space Formulas, *Automatica*, vol.30, no.8, pp.1307-1317, 1994

[22] G.J.Balas, J.C.Doyle, K.Glover, A.Packard, R.Smith: μ-Analysis and Synthesis Toolbox, The MathWorks, 1993

[23] P.Gahinet, A.Nemirovski, A.J.Laub, M.Chilali: LMI Control Toolbox, The MathWorks, 1995